Recombination dynamics of localized excitons in Al 1−x In x N epitaxial films on GaN templates grown by metalorganic vapor phase epitaxy

T. Onuma, SF. Chichibu, Y. Uchinuma, T. Sota, S. Yamaguchi, S. Kamiyama, H. Amano, and I. Akasaki

Citation: Journal of Applied Physics **94**, 2449 (2003); doi: 10.1063/1.1592868
View online: http://dx.doi.org/10.1063/1.1592868
View Table of Contents: http://scitation.aip.org/content/aip/journal/jap/94/4?ver=pdfcov
Published by the AIP Publishing

Recombination dynamics of localized excitons in $Al_{1-x}In_xN$ epitaxial films on GaN templates grown by metalorganic vapor phase epitaxy

T. Onuma, SF. Chichibu,[a] and Y. Uchinuma
Institute of Applied Physics and Graduate School of Pure and Applied Sciences, University of Tsukuba, 1-1-1 Tennodai, Tsukuba 305-8573, Japan

T. Sota
Department of Electrical, Electronics, and Computer Engineering, Waseda University, 3-4-1 Ohkubo, Shinjuku 169-8555, Japan

S. Yamaguchi
Department of Electrical, Electronic and Information Engineering, Kanagawa University, 3-27-1 Rokkakubashi, Kanagawa-ku, Yokohama 221-8686, Japan

S. Kamiyama, H. Amano, and I. Akasaki
High-Tech Research Center, Meijo University, 1-501 Shiogamaguchi, Tempaku-ku, Nagoya 468-8502, Japan

(Received 14 March 2003; accepted 25 May 2003)

Recombination dynamics of excitons in nearly strain-free $Al_{1-x}In_xN$ alloys on the GaN template were studied. Their band-gap energy showed a nonlinear dependence on the InN molar fraction x, and the bowing parameter was determined to be approximately -3.1 eV. Most of the alloys exhibited an extremely diffused band-edge, and consequently exhibited huge Stokes-type shifts up to 1–2 eV and full width at half maximum of the luminescence peaks up to 0.5 eV. The results suggested enhanced material inhomogeneity in AlInN compared to InGaN alloys. Since the time-resolved photoluminescence signal showed a pronounced *stretched exponential* decay, the spontaneous emission was assigned as being due to the radiative recombination of excitons localized in disordered quantum nanostructures. The integrated PL intensity at 300 K was as strong as 29% of that at low temperature, showing a potential use of AlInN alloys as infrared-to-UV light emitters. © *2003 American Institute of Physics.* [DOI: 10.1063/1.1592868]

I. INTRODUCTION

AlInN alloys are a possible candidate for light emitters and detectors operating in extremely wide specrtral regions covering from deep ultraviolet (UV)-to-infrared (IR), since their band-gap energy (E_g) ranges from 6.2 eV (AlN)[1] to 0.7 eV (InN).[2–5] Also, the use of appropriate AlInN enables to fabricate lattice-matched GaN-based heterostructures that can be used for high-performance laser diodes. However, the growth of AlInN alloys is extremely difficult due to the large differences in chemical and physical parameters[6,7] between AlN and InN.

Material properties of AlInN alloys have been studied experimentally[8–16] and theoretically.[17–21] Starosta[8] synthesized AlInN polycrystalline films by reactive multitarget sputtering method. Subsequently, band-gap energy of the alloys has been studied by several researchers[9,12] using such polycrystalline films. However, accurate E_g of single crystal AlInN alloys must be determined, since polycrystalline films often contain oxygen that modifies true E_g. Indeed, E_g of oxygen-free InN has recently been reexamined and determined to be approximately 0.7 eV.[2–5] After Kim *et al.*[11] pointed out that E_g of single crystalline AlInN alloy films grown by metalorganic vapor phase epitaxy (MOVPE) would have large band-gap bowing, Yamaguchi *et al.*[13] grew photoluminescence (PL) properties.[14]

While the number of reports on AlInN alloys is limited, a number of reports on AlGaN and InGaN alloys have been published in the past several years. According to the maturity discussions given for AlGaN and InGaN alloys, a strong internal electric field is considered to exist in strained AlInN alloys due to the spontaneous[22] and piezoelectric[23] polarization along the c axis. The former may be dominant in Al-rich AlInN/GaN structures while the latter may be dominant in In-rich ones if the structure is coherently grown on the GaN base layer. Direction of the total field changes depending on the sign of the piezoelectric field F_{pz} due to the change in the sign of the strain. However, the polarization-induced field in the strain-free thick films may have a negligible contribution, since the spontaneous polarization field, in general, is weakened by the displacement field induced by the free-charge distribution in the material.[22] There is a hypothesis that InGaN alloys contain effective localizing centers for excitons[24] due to the quantum-disk (Qdisk)-size[25] or quantum-dot (QD) size[26–28] effective E_g inhomogeneity. The short length-scale localization of excitons[24,25] has been proposed to prevent them from being trapped in nonradiative defects including threading dislocations, resulting in the increase of the spontaneous emission efficiency (η) at room temperature, which is determined by a competition between the radiative and

[a]Author to whom correspondence should be addressed; also at: Photodynamics Research Center, RIKEN (Institute of Physical and Chemical Research), Aoba, Sendai 980-0845, Japan; electronic mail: optoelec@bk.tsukuba.ac.jp

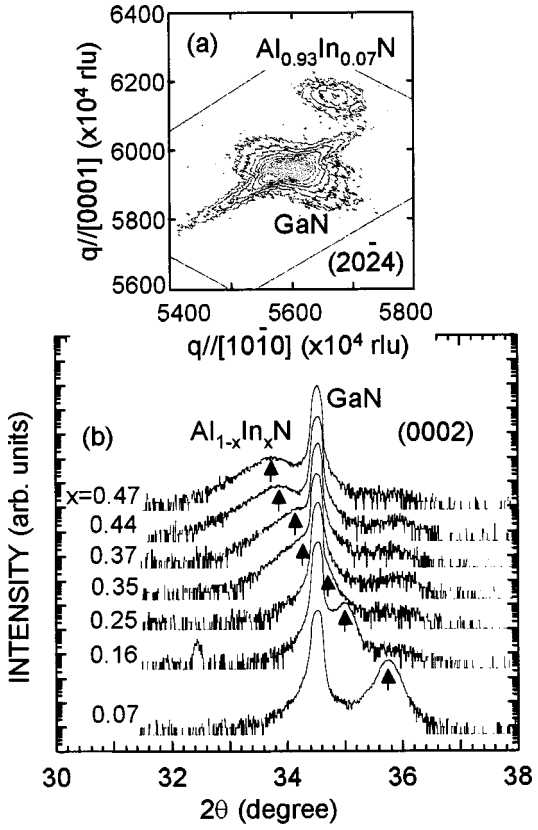

FIG. 1. (a) X-ray reciprocal space mapping near the $(20\bar{2}4)$ diffraction of the $Al_{0.93}In_{0.07}N$ film. (b) θ–2θ diffraction patterns of the $Al_{1-x}In_xN$ films on GaN templates.

nonradiative lifetimes. A similar localization effect can be expected in AlInN alloys, since they contain In in the matrix. Therefore, it is worth investigating the emission mechanisms in AlInN alloys for future realization of integrated multi-wavelength optoelectronic devices.

In this article, results of optical reflectance (OR), PL, cathodoluminescence (CL), and time-resolved PL (TRPL) measurements on nearly strain-free $Al_{1-x}In_xN$ films are shown as functions of InN molar fraction x and temperature T. Spontaneous emission is assigned as being due to the radiative decay of excitons deeply localized in the InN-rich regions.

II. EXPERIMENT

In order to minimize or even remove the effects of polarization field on the intrinsic optical properties in AlInN alloys, 170–660-nm-thick relaxed epitaxial films of $Al_{1-x}In_xN$ ($0.07 \leqslant x \leqslant 0.47$) alloys were prepared on a 2-μm-thick GaN template on (0001) sapphire substrates by MOVPE using a 40-nm-thick low-temperature AlN buffer layer.[13] The sample structure was characterized by high-resolution x-ray diffraction (XRD) technique, and the films are confirmed by a reciprocal space mapping method to be nearly strain free, as shown in Fig. 1(a). Therefore, x is simply calculated from the c lattice parameter obtained from the XRD pattern assuming the Vegard's law. As shown in Fig. 1(b), values of the full width at half maximum (FWHM) of the (0002) diffraction peak are approximately 900 arcsec for $x \leqslant 0.25$, and then increase linearly with x for $x \geqslant 0.25$. The result indicates enhanced compositional fluctuation as well as strain fluctuation.

OR spectra were measured with an incident angle smaller than 25°. A white light from a Xe or a halogen lamp was irradiated, depending on the wavelength to be observed. Steady-state PL was excited by a 242 nm beam of a quasi-continuous wave frequency-tripled Ti:Sapphire laser, and CL was excited by an electron beam with an acceleration energy of 2 keV. Reflected light for the OR measurement, PL, and CL were dispersed by a grating monochromator and detected phase sensitively by a UV-visible or a solar-blind photomultiplier. TRPL was excited by a 80 fs pulse of a frequency-tripled mode-locked Ti:Sapphire laser, and the signal was collected using a standard streak-camera data acquisition system. The minimum time resolution was approximately 15 ps.

III. RESULTS AND DISCUSSION

A. Steady-state optical spectra of AlInN films

OR spectra of the $Al_{1-x}In_xN$ films measured at 8 K are shown in Fig. 2. The spectra exhibit two independent multiple interference fringes having shorter and longer periods, which are due to the internal reflection in GaN base layer and AlInN layer, respectively. In general, OR spectrum of direct band-gap semiconductor thin films exhibits excitonic reflectance anomalies[29] just above the photon energy at which multiple interference fringes vanish. Indeed, OR spectrum of the 2-μm-thick AlN film has exhibited[30] a combined free A- and B-excitonic reflectance anomalies, as shown in the inset of Fig. 2. However, such structures cannot be seen in the alloy films due to the broad band-edge. Therefore, effective E_g of AlInN is determined as the higher-energy edge of the longer period reflection fringes. The energy position of E_g is marked by the arrows, and the values are plotted by closed triangles in Fig. 3 as a function of x. The bowing parameter b in the strain-free $Al_{1-x}In_xN$ films is thus determined to be -3.1 eV assuming the quadratic dependence of E_g on x, as shown by the solid line in Fig. 3. In the fitting, E_g of AlN and InN at low temperature are taken as 6.28 (Refs. 30 and 31) and 0.7 eV,[2–5] respectively. The value of $b=-3.1$ eV is consistent with that obtained by the first-principles calculation (-1.32–-3.326 eV).[17,18,20,21]

PL and CL spectra exhibit broad emission bands, as shown in Fig. 2. The luminescence peak energies are plotted by open circles in Fig. 3. Note that the CL peak energy for the $Al_{0.93}In_{0.07}N$ film is tentatively plotted allowing large uncertainty, since the emission band due to AlInN is overlapped with that from the GaN template (3.4 eV), as shown by the upward arrow in Fig. 2. The Stokes-type shifts (SS) are as large as 1–2 eV and the values of FWHM for the emissions are as large as 0.5 eV, as shown in Fig. 3. Obviously, these large FWHM values cannot be explained by the classical alloy broadening model[32] for all samples. The results may reflect the incongruent nature of AlN and InN due to the poor solubility.[6,7]

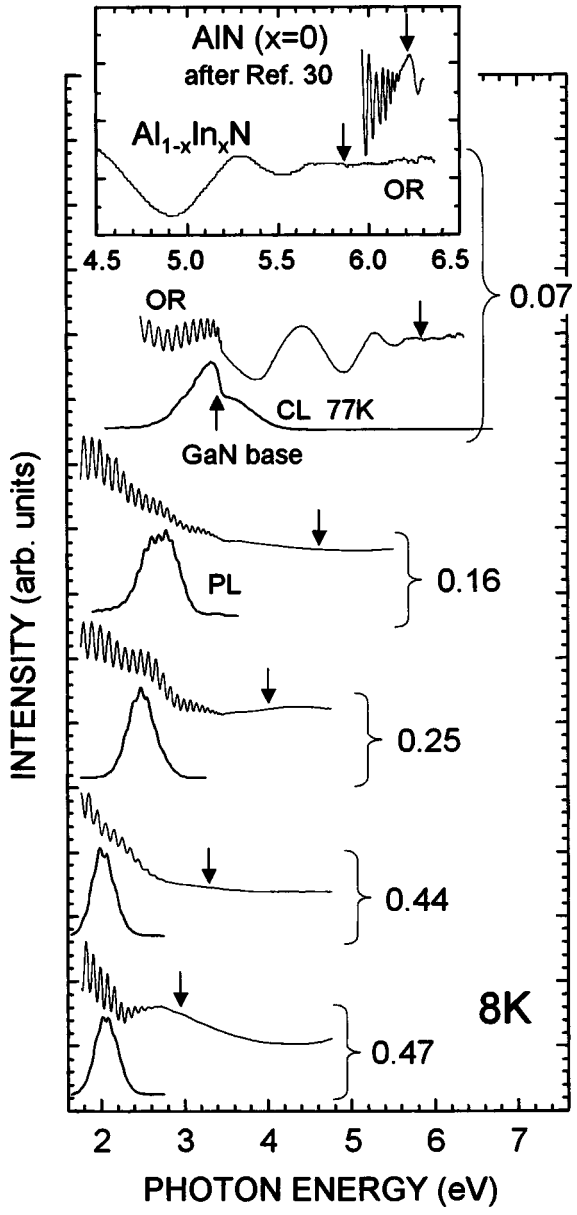

FIG. 2. OR, PL, and CL spectra of strain-free $Al_{1-x}In_xN$ films. The downward arrows indicate the energy position of E_g. The OR spectrum of a 2-μm-thick AlN film (after Ref. 30) is shown in the inset for comparison. A luminescence peak at 3.4 eV marked by the upward arrow in the CL spectrum of $Al_{0.93}In_{0.07}N$/GaN structure is due to the emission from the GaN template.

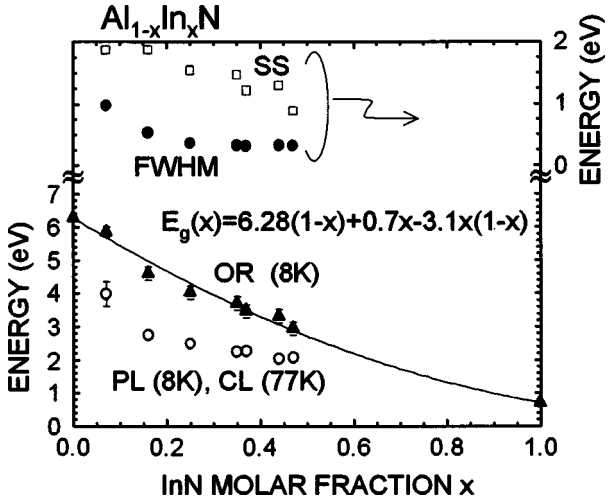

FIG. 3. Values of E_g (closed triangle) derived from OR spectrum, emission peak energy (open circle), SS (open square), and FWHM of the emissions (closed circle) as a function of x.

B. Recombination dynamics in AlInN films

TRPL signals at the peak energies for the $Al_{0.56}In_{0.44}N$ film are shown as a function of T in Fig. 4. The signal shows a pronounced *stretched exponential* decay[33,34] from 8 K up to 300 K. The decay curve is therefore fitted using the model exciton localization into disordered quantum nanostructures,[35] as has been carried out for InN clusters, QDs, or Qdisk-size potential fluctuation in both wurtzite and zincblende InGaN alloys.[36–38] The $\ln\{\ln[I_0/I(t)]\}$ versus $\ln(t)$ relation for the decay curve $I(t)=I_0\exp[-(t/\tau_{\text{ini}})^{\beta}]$ at 8 K is plotted in Fig. 5(a), where $I(t)$ is the PL intensity at time t, I_0 is $I(0)$, β is the scaling parameter that is considered to be related to the dimensionality of the localizing centers, and τ_{ini} is the initial lifetime. The linear fit gives $\beta=0.73$ and $\tau_{\text{ini}}=57$ ps. Different from the results for AlGaN or InGaN, the energy-resolved decay shape does not change as the detection (emission) photon energy is changed; i.e., spectral diffusion is not seen. The results indicate that excitons recombine at deep localizing centers having fractal dimensions, and the cross relaxation within the tail states is not really effective. The physical meaning of this is that AlInN has an extremely extended band-edge similar to that of amorphous materials.

In the localized exciton system, improvement of the internal quantum efficiency, η_{int}, compared to that of free exciton or band-to-band emission at 300 K is expected, as observed in InGaN alloys.[24] Indeed, the integrated PL intensity of the $Al_{0.56}In_{0.44}N$ film at 300 K is as strong as 29% of that

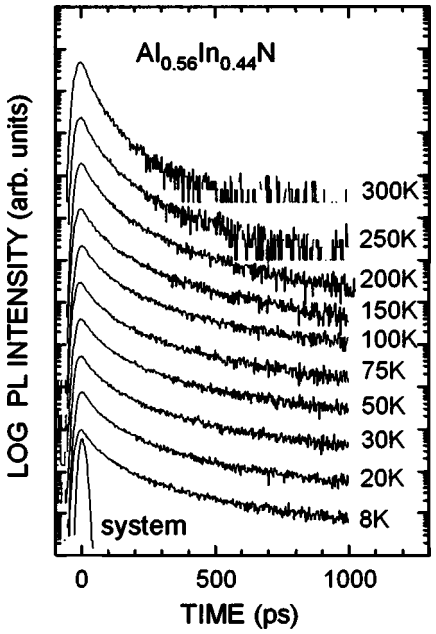

FIG. 4. TRPL signals of the $Al_{0.56}In_{0.44}N$ film as a function of T.

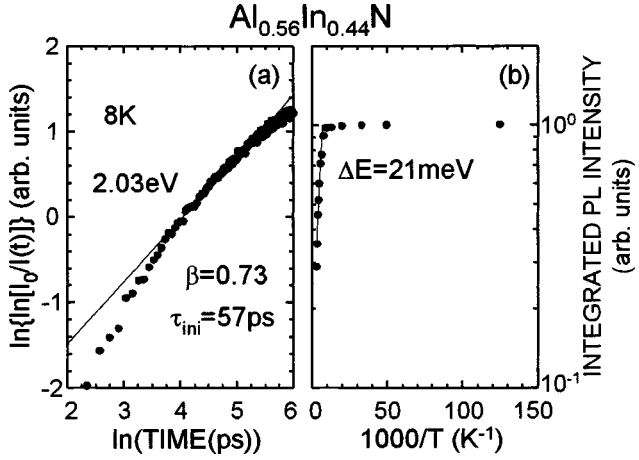

FIG. 5. (a) $\ln\{\ln[I_0/I(t)]\}$ vs $\ln(t)$ relation for the TRPL signal of the $Al_{0.56}In_{0.44}N$ film at 8 K. (b) The integrated PL intensity as a function of T. The thermal activation energy of $\Delta E = 21$ meV above 150 K corresponds to the effective activation energy of nonradiative recombination channels.

at 8 K, as shown in Fig. 5(b). The PL lifetime τ_{PL} decreases remarkably above 200 K, as shown in Fig. 4. In order to analyze the role of radiative and nonradiative processes as functions of x and T, the PL lifetime τ_{PL}, which refers τ_{ini} at the PL peak energy, of the $Al_{1-x}In_xN$ films with $x=0.25$ and 0.44 are plotted by closed triangles in Figs. 6(a) and 6(b), respectively. Since the excitons are transferred from the *free* or *extended* states to the localizing centers before the radiative decay in the present AlInN alloys, the data are analyzed by the simplified three-level localized exciton model[39] that was used to analyze the emission characteristics in cubic (c-) InGaN alloys. In the model, the *localization lifetime* (τ_{loc}) was introduced to express the *transfer and radiative* combined lifetime of excitons in efficiently localized electronic systems, where τ_{loc} is inversely proportional to the capturing rate minus escaping rate of excitons between the *free/extended* states and localizing centers. It increases with

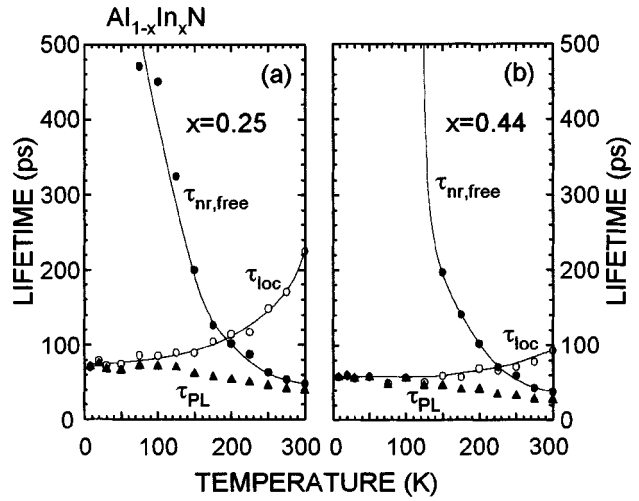

FIG. 6. PL lifetime τ_{PL} (closed triangle) of (a) $Al_{0.75}In_{0.25}N$ and (b) $Al_{0.56}In_{0.44}N$ films as a function of T. The localization lifetime τ_{loc} (open circle) and the nonradiative lifetime at the *free/extended* states $\tau_{nr,free}$ (closed circle) derived from τ_{PL} and corresponding integrated PL intensity as a function of T.

T and the occupancy of the localizing centers while it decreases with the increase in localization depth E_{loc}. Details of the model will be found elsewhere.[39] Values of τ_{loc} and nonradiative lifetime in the *free/extended* states ($\tau_{nr,free}$) are deduced from τ_{PL} and η_{int} as a function of T [see Fig. 5(b)] using the relation $\eta_{int}=1/(1+\tau_{loc}/\tau_{nr,free})$. Note that η_{int} is assumed to be unity at low temperature, since the nonradiative process is generally frozen.

Values of τ_{loc} and $\tau_{nr,free}$ are plotted as a function of T in Figs. 6(a) and 6(b). The magnitude of τ_{loc} for our AlInN alloys is several tenths of ps at low temperature and 100–200 ps at 300 K. These values are shorter than that of c-InGaN quantum wells,[39] showing the strongly localized nature of excitons in AlInN. Moreover, the $Al_{0.56}In_{0.44}N$ film exhibits shorter τ_{loc} compared to $Al_{0.75}In_{0.25}N$ one for entire temperature range. The result indicates *fast* exciton localization due to the increase in the effective localization depth with x for $x \geqslant 0.25$. On the other hand, $\tau_{nr,free}$ of the $Al_{0.56}In_{0.44}N$ film decreases more rapidly than that of the $Al_{0.75}In_{0.25}N$ film at higher temperature; the value of $\tau_{nr,free}$ for the $Al_{0.56}In_{0.44}N$ film at 300 K ($\sim$35 ps) is smaller than that for the $Al_{0.75}In_{0.25}N$ film ($\sim$50 ps). The result indicates the increase of nonradiative defect density in the *free/extended* states with the increase in x for $x \geqslant 0.25$. However, η_{int} for the $Al_{0.56}In_{0.44}N$ film at 300 K is as high as 29% [see Fig. 5(b)] compared to that for the $Al_{0.75}In_{0.25}N$ film (17%), reflecting the defect-resistant nature of effective localization mechanisms.

IV. CONCLUSION

Spontaneous emission mechanisms in strain-free $Al_{1-x}In_xN$ films on GaN templates were studied. They exhibited a large band-gap bowing with a bowing parameter of approximately -3.1 eV. The TRPL signals showed a *stretched exponential* decay up to 300 K, indicating that the emission is due to the radiative recombination of deeply localized excitons in disordered quantum nanostructures. Since η_{int} of the present defective AlInN films is still as high as 29% at 300 K, realization of UV and IR light emitters can be expected due to further reduction of the nonradiative defect density in the *free/extended* states.

ACKNOWLEDGMENTS

The authors are grateful to Dr. H. Okumura of AIST for providing CL apparatus, and to K. Torii and K. Hazu of Waseda University for help in the TRPL measurements. This work was supported in part by the 21st Century COE programs ''Promotion of Creative Interdisciplinary Materials Science for Novel Functions'' at the University of Tsukuba and ''Nano-Factory'' at Meijo University under MEXT Japan, Akasaki Research Center, Nagoya University, Sasagawa Scientific Research Grant from The Japan Science Society, and AOARD/AFOSR.

[1] W. M. Yim, E. J. Stofko, P. J. Zanzucchi, J. I. Pankove, M. Ettenbergm, and S. L. Gilbert, J. Appl. Phys. **44**, 292 (1973).
[2] T. Inushima, V. V. Mamutin, V. A. Vekshim, S. V. Ivanov, T. Sakon, M. Motokawa, and S. Ohoya, J. Cryst. Growth **227-228**, 481 (2001).
[3] V. Y. Davydov, A. A. Klochikhin, R. P. Seisyan, V. V. Emtsev, S. V.

Ivanov, F. Bechstedt, J. Furthmüller, H. Harima, A. V. Mudryi, J. Aderhold, O. Semchinova, and J. Graul, Phys. Status Solidi B **229**, R1 (2002).
[4] J. Wu, W. Walukiewicz, K. M. Yu, J. W. Ager III, E. E. Haller, H. Lu, W. J. Schaff, Y. Saito, and Y. Nanishi, Appl. Phys. Lett. **80**, 3967 (2002).
[5] T. Matsuoka, H. Okamoto, M. Nakao, H. Harima, and E. Kurimoto, Appl. Phys. Lett. **81**, 1246 (2002).
[6] A. Koukitu and H. Seki, Jpn. J. Appl. Phys., Part 2 **35**, L1638 (1996).
[7] T. Matsuoka, Appl. Phys. Lett. **71**, 105 (1997).
[8] K. Starosta, Phys. Status Solidi A **68**, K55 (1981).
[9] K. Kubota, Y. Kobayashi, and K. Fujimoto, J. Appl. Phys. **66**, 2984 (1989).
[10] Q. Guo, H. Ogawa, and A. Yoshida, J. Cryst. Growth **146**, 462 (1995); Jpn. J. Appl. Phys., Part 1 **34**, 4653 (1995).
[11] K. S. Kim, A. Saxler, P. Kung, M. Razaghi, and K. Y. Lim, Appl. Phys. Lett. **71**, 800 (1997).
[12] T. Peng, J. Piprek, G. Qiu, J. O. Olowoiafe, K. M. Unruh, C. P. Swann, and E. F. Shubert, Appl. Phys. Lett. **71**, 2439 (1997).
[13] S. Yamaguchi, M. Kariya, S. Nitta, H. Kato, T. Takeuchi, C. Wetzel, H. Amano, and I. Akasaki, J. Cryst. Growth **195**, 309 (1998); M. Kariya, S. Nitta, S. Yamaguchi, H. Kato, T. Takeuchi, C. Wetzel, H. Amano, and I. Akasaki, Jpn. J. Appl. Phys., Part 2 **37**, L697 (1998).
[14] S. Yamaguchi, M. Kariya, S. Nitta, T. Takeuchi, C. Wetzel, H. Amano, and I. Akasaki, Appl. Phys. Lett. **73**, 830 (1998); *ibid.* **76**, 876 (2000).
[15] T. V. Shubina, V. V. Mamutin, V. A. Vekshin, V. V. Ratnikov, A. A. Toropov, A. A. Sitnikova, S. V. Ivanov, M. Karlsteen, U. Södervall, M. Willander, G. Pozina, J. P. Bergman, and B. Monemar, Phys. Status Solidi B **216**, 205 (1999).
[16] M. J. Lukitsch, Y. V. Danylyuk, V. M. Naik, C. Huang, G. W. Auner, L. Rimai, and R. Naik, Appl. Phys. Lett. **79**, 632 (2001).
[17] A. F. Wright and J. S. Nelson, Appl. Phys. Lett. **66**, 3465 (1995).
[18] M. Goano, E. Bellotti, E. Ghillino, C. Garetto, G. Ghione, and K. F. Brennan, J. Appl. Phys. **88**, 6476 (2000).
[19] M. Ferhat and F. Bechstedt, Phys. Rev. B **65**, 075213 (2002).
[20] Y.-K. Kuo and W.-W. Lin, Jpn. J. Appl. Phys., Part 1 **41**, 5557 (2002).
[21] L. K. Teles, L. M. R. Scolfaro, J. Furthmüller, F. Bechstedt, and J. R. Leite, Phys. Status Solidi B **234**, 956 (2002); J. Appl. Phys. **92**, 7109 (2002).
[22] F. Bernardini and V. Fiorentini, Phys. Rev. B **57**, R9427 (1998); Phys. Status Solidi B **216**, 391 (1999).
[23] T. Takeuchi, S. Sota, M. Katsuragawa, M. Komori, H. Takeuchi, H. Amano, and I. Akasaki, Jpn. J. Appl. Phys., Part 2 **36**, L382 (1997).
[24] S. Chichibu, T. Azuhata, T. Sota, and S. Nakamura, Appl. Phys. Lett. **69**, 4188 (1996).
[25] S. Chichibu, K. Wada, and S. Nakamura, Appl. Phys. Lett. **71**, 2346 (1997).
[26] Y. Narukawa, Y. Kawakami, M. Funato, Sz. Fujita, Sg. Fujita, and S. Nakamura, Appl. Phys. Lett. **70**, 981 (1997).
[27] C. Kisielowski, Z. Liliental-Weber, and S. Nakamura, Jpn. J. Appl. Phys., Part 1 **36**, 6932 (1997).
[28] K. P. O'Donnell, R. W. Martin, and P. G. Middleton, Phys. Rev. Lett. **82**, 237 (1999); R. W. Martin, P. G. Middleton, K. P. O'Donnell, and W. Van der Stricht, Appl. Phys. Lett. **74**, 263 (1999).
[29] D. E. Aspnes, Surf. Sci. **37**, 418 (1973).
[30] T. Onuma, S. F. Chichibu, T. Sota, K. Asai, S. Sumiya, T. Shibata, and M. Tanaka, Appl. Phys. Lett. **81**, 652 (2002).
[31] P. B. Perry and R. F. Rutz, Appl. Phys. Lett. **33**, 319 (1978).
[32] E. F. Schubert, E. O. Göbel, Y. Horikoshi, K. Ploog, and H. J. Queisser, Phys. Rev. B **30**, 813 (1984).
[33] L. Pavesi and M. Ceschini, Phys. Rev. B **48**, 17625 (1993).
[34] A. Y. Kobitski and K. S. Zhuravlev, Phys. Rev. B **63**, 115423 (1993).
[35] X. Chen, B. Henderson, and K. P. O'Donnell, Appl. Phys. Lett. **60**, 2672 (1992).
[36] M. Pophristic, F. H. Long, C. Tran, I. T. Ferguson, and R. F. Karlicek, Jr., Appl. Phys. Lett. **73**, 3550 (1998).
[37] J. Holst, A. Hoffmann, D. Rudloff, F. Bertram, T. Riemann, J. Christen, T. Frey, D. As, D. Schikora, and K. Lischka, Appl. Phys. Lett. **76**, 2832 (2000).
[38] S. F. Chichibu, M. Sugiyama, T. Kuroda, A. Tackeuchi, T. Kitamura, H. Nakanishi, T. Sota, S. P. DenBaars, S. Nakamura, Y. Ishida, and H. Okumura, Appl. Phys. Lett. **79**, 3600 (2001); S. F. Chichibu, M. Sugiyama, T. Onuma, T. Kitamura, H. Nakanishi, T. Kuroda, A. Tackeuchi, T. Sota, Y. Ishida, and H. Okumura, *ibid.* **79**, 4319 (2001).
[39] SF. Chichibu, T. Onuma, T. Sota, S. P. DenBaars, S. Nakamura, T. Kitamura, Y. Ishida, and H. Okumura, J. Appl. Phys. **93**, 2051 (2003); the *localization lifetime* τ_{loc} represents the combined *transfer and radiative* lifetime of excitons, which increases with temperature T and occupancy of the localized states and decreases with the increase in the localization depth E_{loc}.